Inorg. Chem. **2006**, *45*, 9729–9741

Photophysical Properties of Ruthenium(II) Tris(2,2′-bipyridine) Complexes Bearing Conjugated Thiophene Appendages

Anthony Harriman,*,† Guillaume Izzet,† Sébastien Goeb,‡ Antoinette De Nicola,‡ and Raymond Ziessel*,‡

Molecular Photonics Laboratory, School of Natural Sciences, Bedson Building, University of Newcastle, Newcastle upon Tyne, NE1 7RU, United Kingdom, and Laboratoire de Chimie Moléculaire, Ecole Européenne de Chimie, Polymères et Matériaux, Université Louis Pasteur, 25 rue Becquerel, 67087 Strasbourg Cedex 02, France

Received May 26, 2006

A small series of ruthenium(II) tris(2,2′-bipyridine) complexes has been synthesized in which ethynylated thiophene residues are attached to one of the 2,2′-bipyridine ligands. The photophysical properties depend on the conjugation length of the thiophene-based ligand, and in each case, dual emission is observed. The two emitting states reside in thermal equilibrium at ambient temperature and can be resolved by emission spectral curve-fitting routines. This allows the properties of the two states to be evaluated in both fluid butyronitrile solution and a transparent KBr disk. It is concluded that both emitting states are of metal-to-ligand charge-transfer (MLCT) character, and despite the presence of conjugated thiophene residues, there is no indication for a low-lying π,π^*-triplet state that promotes nonradiative decay of the excited-state manifold. A key feature of these systems is that the conjugation length imposed by the thiophene-based ligand helps to control the rate constants for both radiative and nonradiative decay from the two MLCT triplet states.

Introduction

A large number of ruthenium poly(pyridine) complexes have been synthesized in which an aromatic polycycle is appended close to the metal complex.[1] Such derivatives have been highly successful as a strategy for prolonging the lifetime of the lowest-energy triplet excited state associated with the metal complex.[2−4] Indeed, triplet lifetimes have been increased from a few microseconds to more than 100 μs in certain cases.[2,3] The most popular polycycle has been pyrene, and a wide variety of such derivatives are now known.[1] Prolongation of the triplet lifetime results from the rapid establishment of a thermally equilibrated mixture of triplet states and requires that the triplet states resident on metal complex and polycycle are almost isoenergetic.[5] A similar approach has been used with osmium(II) poly(pyridine) complexes[6] and employed for the construction of multinuclear metal complexes.[2]

Recently, a new application for this same synthetic strategy has evolved.[7] Thus, considerable attention has focused on the design of metal poly(pyridine)-based systems able to transfer triplet energy over unusually long distances.[8] This

* To whom correspondence should be addressed. E-mail: anthony.harriman@ncl.ac.uk (A.H.); ziessel@chimie.u-strasbg.fr (R.Z.).
† University of Newcastle.
‡ Université Louis Pasteur.

(1) Harriman, A.; Ziessel, R. In *Carbon-Rich Compounds*; Haley, M. M., Tykwinski, R. R., Eds.; Wiley-VCH: Weinheim, Germany, 2006; pp 26−89.
(2) Harriman, A.; Khatyr, A.; Ziessel, R. *Dalton Trans*. **2003**, 2061.
(3) (a) Hissler, M.; Harriman, A.; Khatyr, A.; Ziessel, R. *Chem.—Eur. J.* **1999**, *5*, 3366. (b) Harriman, A.; Hissler, M.; Khatyr, A.; Ziessel, R. *Chem. Commun.* **1999**, *8*, 735. (c) Tyson, D. S.; Bialecki, J.; Castellano, F. N. *Chem. Commun.* **2000**, 2355. (d) Leroy-Lhez, S.; Belin, C.; D'aleo, A.; Williams, R. M.; De Cola, L.; Fages, F. *Supramol. Chem.* **2003**, *15*, 627. (e) Tyson, D. S.; Luman, C. R.; Zhou, X.; Castellano, F. N. *Inorg. Chem.* **2001**, *40*, 4063. (f) Kozlov, D. V.; Tyson, D. S.; Goze, C.; Ziessel, R.; Castellano, F. N. *Inorg. Chem.* **2004**, *43*, 6083. (g) Tyson, D. S.; Castellano, F. N. *J. Phys. Chem. A* **1999**, *103*, 10955.
(4) (a) McClenaghan, N. D.; Barigelletti, F.; Maubert, B.; Campagna, S. *Chem. Commun.* **2002**, 602. (b) Medlycott, E. A.; Hanan, G. S. *Chem. Soc. Rev.* **2005**, *34*, 133. (c) Ioachim, E.; Medlycott, E. A.; Hanan, G. S.; Loiseau, F.; Campagna, S. *Inorg. Chim. Acta* **2006**, *359*, 766. (d) Wang, Y.; Liu, S.; Pinto, M. R.; Dattelbaum, D. M.; Schoonover, J. R.; Schanze, K. S. *J. Phys. Chem. A* **2001**, *105*, 11118.
(5) (a) Ford, W. E.; Rodgers, M. A. J. *J. Phys. Chem.* **1992**, *96*, 2917. (b) Wilson, G. J.; Sasse, W. H. F.; Mau, A. W.-H. *Chem. Phys. Lett.* **1996**, *250*, 583. (c) Wilson, G. J.; Launikonis, A.; Sasse, W. H. F.; Mau, A. W.-H. *J. Phys. Chem. A* **1997**, *101*, 4860.
(6) (a) El-ghayoury, A.; Harriman, A.; Ziessel, R. *Chem. Commun.* **1999**, *20*, 2027. (b) Benniston, A. C.; Harriman, A.; Li, P.; Sams, C. A. *J. Phys. Chem. A* **2005**, *109*, 2302.
(7) Harriman, A.; Rostron, S. A.; Khatyr, A.; Ziessel, R. *Faraday Discuss.* **2006**, *131*, 377.

10.1021/ic060921w CCC: $33.50 © 2006 American Chemical Society
Published on Web 10/26/2006

Chart 1. Structural Formulas and Abbreviations Used for the Thiophene-Functionalized Ruthenium(II) Tris(2,2′-bipyridine) Complexes Studied in This Work[a]

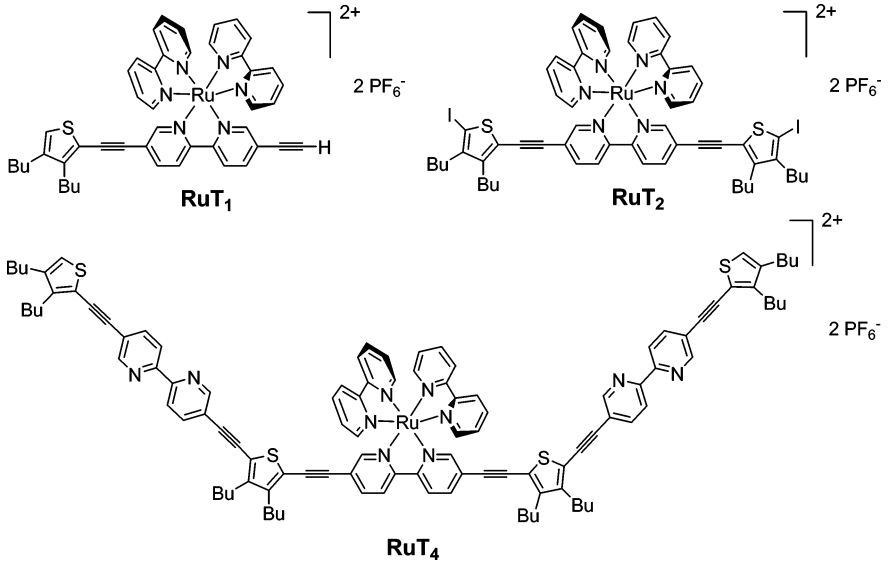

[a] Note that each complex is dicationic and that two PF_6^- anions are associated with each structure.

work has involved the attachment of different metal complexes to either end of a molecular-scale bridge constructed by the stepwise oligomerization of individual modules into a linear structure.[1] The rate of triplet energy transfer between the terminals depends on the length and composition of the bridge. At first, interest was directed to those bridges where the triplet energy of the donor was well below that of the bridge, the so-called super-exchange mechanism, and several effective bridges have been identified.[9] Notable among the putative building blocks have been ethynylated aromatic groups.[10] The alternative design principle, the so-called hopping mechanism, uses a donor whose triplet energy is slightly above that of the bridge.[11] Here, illumination of the donor results in injection of triplet energy into the bridge, followed by energy migration and subsequent trapping by the acceptor. This approach can provide for very fast rates of triplet energy transfer regardless of the length of the bridge.[12] It is necessary, however, to identify suitable molecular-scale connectors.[1]

Here, we consider the photophysical properties of a small series of ruthenium(II) tris(2,2′-bipyridine) complexes bearing an attached π-conjugated aryl chain (Chart 1). The chain comprises a thiophene residue, known to be a good conduit for long-range electronic coupling,[13] attached to the 2,2′-bipyridine ligand via an ethynylene group. Related structures[14] have been found to display efficient exciton transfer over distances in excess of 30 Å via the charge hopping mechanism. The intention of the present work is to clarify the nature of the lowest-energy excited triplet state in such systems, with particular reference to the relative energies of ligand-centered and metal complex-localized excited states,[15] and to evaluate the temperature dependence for any luminescence emanating from the equilibrated system. This latter

(8) (a) Balzani, V.; Scandola, F. *Supramolecular Photochemistry*; Horwood: Chichester, U.K., 1991. (b) Benniston, A. C.; Grosshenny, V.; Harriman, A.; Ziessel, R. *Angew. Chem., Int. Ed. Engl.* **1994**, *33*, 1884. (c) Harriman, A.; Khatyr, A.; Ziessel, R.; Benniston, A. C. *Angew. Chem., Int. Ed*. **2000**, *39*, 4287. (d) Welter, S.; Lafolet, F.; Cecchetto, E.; Vergeer, F.; De Cola, L. *Chem. Phys. Chem.* **2005**, *6*, 2417. (e) Flores-Torres, S.; Hutchison, G. R.; Soltzberg, L. J.; Abruna, H. D. *J. Am. Chem. Soc.* **2006**, *128*, 1513.

(9) (a) Eng, M. P.; Ljungdahl, T.; Mårtensson, J.; Albinsson, B. *J. Phys. Chem. B* **2006**, *110*, 6483. (b) Benniston, A. C.; Harriman, A.; Li, P.; Sams, C. A. *J. Am. Chem. Soc.* **2005**, *127*, 2553. (c) Chiorboli, C.; Fracasso, S.; Ravaglia, M.; Scandola, F.; Campagna, S.; Wouters, K. L.; Konduri, R.; MacDonnell, F. M. *Inorg. Chem*. **2005**, *44*, 8368. (d) Welter, S.; Salluce, N.; Belser, P.; Groeneveld, M.; De Cola, L. *Coord. Chem. Rev.* **2005**, *249*, 1360. (e) Welter, S.; Salluce, N.; Benetti, A.; Rot, N.; Belser, P.; Sonar, P.; Grimsdale, A. C.; Mullen, K.; Lutz, M.; Spek, A. L.; De Cola, L. *Inorg. Chem.* **2005**, *44*, 4706. (f) Guckian, A. L.; Doering, M.; Ciesielski, M.; Walter, O.; Hjelm, J.; O'Boyle, N. M.; Henry, W.; Browne, W. R.; McGarvey, J. J.; Vos, J. G. *Dalton Trans*. **2004**, 3943. (g) Constable, E. C.; Handel, R. W.; Housecroft, C. E.; Morales, A. F.; Flamigni, L.; Barigelletti, F. *Dalton Trans*. **2003**, 1220. (h) Akasaka, T.; Inoue, H.; Kuwabara, M.; Mutai, T.; Otsuki, J.; Araki, K. *Dalton Trans*. **2003**, 815. (i) Beyeler, A.; Belser, P. *Coord. Chem. Rev.* **2002**, *230*, 29. (j) Baudin, H. B.; Davidsson, J.; Serroni, S.; Juris, A.; Balzani, V.; Campagna, S.; Hammarström, L. *J. Phys. Chem. A* **2002**, *106*, 4312. (k) Ward, M. D.; Barigelletti, F. *Coord. Chem. Rev.* **2001**, *216*, 127.

(10) (a) Grosshenny, V.; Harriman, A.; Ziessel, R. *Angew. Chem., Int. Ed. Engl.* **1996**, *34*, 2705. (b) Hissler, M.; El-ghayoury, A.; Harriman, A.; Ziessel, R. *Angew. Chem., Int. Ed. Engl.* **1998**, *37*, 1717. (c) Benniston, A. C.; Harriman, A.; Grosshenny, V.; Ziessel, R. *New J. Chem.* **1997**, *21*, 405.

(11) (a) El-ghayoury, A.; Harriman, A.; Ziessel, R. *J. Phys. Chem. A* **2000**, *104*, 7906. (b) El-ghayoury, A.; Harriman, A.; Khatyr, A.; Ziessel, R. *J. Phys. Chem. A* **2000**, *104*, 1512. (c) Khatyr, A.; Ziessel, R. *J. Org. Chem.* **2000**, *65*, 3126.

(12) (a) Muller, J. G.; Atas, E.; Tan, C.; Schanze, K. S.; Kleiman, V. D. *J. Am. Chem. Soc.* **2006**, *128*, 4007. (b) Dias, F. B.; Knaapila, M.; Monkman, A. P.; Burrows, H. D. *Macromolecules* **2006**, *39*, 1598. (c) Chaignon, F.; Torroba, J.; Blart, E.; Borgström, M.; Hammarström, L.; Odobel, F. *New J. Chem.* **2005**, *29*, 1272. (d) Sancho-García, J. C.; Brédas, J. L.; Beljonne, D.; Cornil, J.; Martínez-Álvarez, R.; Hanack, M.; Poulsen, L.; Gierschner, J.; Mack, H.-G.; Egelhaaf, H. J.; Oelkrug, D. *J. Phys. Chem. B* **2005**, *109*, 4872.

(13) (a) Mikroyannidis, J. A.; Spiliopoulos, I. K.; Kulkarni, A. P.; Jenekhe, S. A. *Synth. Met.* **2004**, *142*, 113. (b) Skabara, P. J.; Berridge, R.; McInnes, E. J. L.; West, D. P.; Coles, S. J.; Hursthouse, M. B.; Mullen, K. *J. Mater. Chem*. **2004**, *14*, 1964.

(14) (a) Ziessel, R.; Bäuerle, P.; Ammann, M.; Barbieri, A.; Barigelletti, F. *Chem. Commun*. **2005**, 802. (b) Goeb, S.; De Nicola, A.; Ziessel, R.; Sabatini, C.; Barbieri, A.; Barigelletti, F. *Inorg. Chem.* **2006**, *45*, 1173.

feature is an important tool for examining energy gaps and injection rates. A long-term goal of the work is to devise improved pathways for very long-range triplet energy transfer.

Experimental Methods

Structural formulas for the molecular systems studied herein are given in Chart 1; the abbreviations are intended to convey the number of attached thiophene residues. The new compounds were synthesized by conventional methods using well-defined precursors and characterized by ^{1}H and ^{13}C NMR, FT-IR, UV−vis spectroscopy, ES-MS, and elemental analysis. The key building blocks were prepared according to literature procedures.[16]

Synthesis and Characterization. 5-[(3,4-Dibutylthien-2-yl)-ethynyl]-5′-ethynyl-2,2′-bipyridine (T_1). A mixture of KF (198 mg, 3.41 mmol) in H_2O (5 mL) was added to a solution of 5-[(3,4-dibutylthien-2-yl)ethynyl]-5′-(triethylsilyl)ethynyl-2,2′-bipyridine **T_1-(TES)**[16] (350 mg, 0.68 mmol) in THF (20 mL) and MeOH (10 mL). The solution was stirred for 3 h, and then the solvent was evaporated under vacuum. The residue was treated with water and extracted with dichloromethane. The organic extracts were washed with water and then brine and dried over magnesium sulfate. The solvent was removed by rotary evaporation. The residue was purified by chromatography on alumina, eluting with dichloromethane−hexane (v/v 10/90), to give 231 mg of **T_1** (84%) as a colorless viscous liquid. ^{1}H NMR (200 MHz, $CDCl_3$): δ 8.75 (m, 2H), 8.39 (m, 2H), 7.87 (m, 2H), 7.23 (s, 1H), 3.30 (s, 1H), 2.74 (m, 2H), 2.52 (m, 2H), 1.50 (m, 8H), 0.93 (m, 6H). ^{13}C NMR (50 MHz, $CDCl_3$): δ 154.7, 153.6, 152.2, 151.2, 147.9, 142.2, 139.9, 138.7, 122.4, 120.9, 120.6, 120.4, 119.2, 117.7, 91.8, 88.0, 81.5, 80.7, 32.2, 31.9, 28.7, 28.0, 22.7, 22.6, 14.0. IR (KBr, cm^{-1}): 3051, 2956, 2927, 2857, 2200, 1636, 1587, 1529, 1464. FAB$^+$ (nature of the peak, relative intensity): *m/z* 399.1 ([M + H]$^+$, 100). Anal. Calcd for $C_{26}H_{26}N_2S$: C, 78.35; H, 6.58; N, 7.03. Found: C, 78.20; H, 6.30; N, 6.68.

RuT_1(TES). $[Ru(bpy)_2Cl_2]\cdot 2H_2O$ (56 mg, 0.11 mmol) was added to a mixture of 5-[(3,4-dibutylthien-2-yl)ethynyl]-5′-(triethylsilyl)-ethynyl-2,2′-bipyridine (**T_1(TES)**, 50 mg, 0.10 mmol) in EtOH (10 mL). The mixture was heated at 90 °C for 12 h, and then the solvent was evaporated under vacuum. The residue was treated with a satured solution of KPF_6 and extracted with dichloromethane. The organic extracts were washed with water and dried over absorbent cotton. The solvent was removed by rotary evaporation. The residue was purified by chromatography on alumina, eluting with dichloromethane−hexane (v/v 50/50) to dichloromethane−methanol (v/v 98/2), to give 97 mg (82%) of **RuT_1(TES)** as an orange solid. ^{1}H NMR (400.1 MHz, $(CD_3)_2CO$): δ 8.84−8.78 (m, 6H), 8.27−8.17 (m, 8H), 8.09−8.06 (m, 3H), 7.92 (s, 1H), 7.63−7.58 (m, 4H), 7.25 (s, 1H), 2.64 (t, 2H, ^3J = 7.5 Hz), 2.55 (t, 2H, ^3J = 7.5 Hz), 1.64−1.27 (m, 8H), 0.94 (t, 9H, ^3J = 8.0 Hz), 0.92 (t, 3H, ^3J = 7.5 Hz), 0.88 (t, 3H, ^3J = 7.5 Hz), 0.62 (q, 6H, ^3J = 7.5 Hz). ^{13}C NMR (100.6 MHz, $(CD_3)_2CO$): δ 158.2, 158.0, 157.9, 157.0, 156.0, 154.6, 153.6, 153.2, 152.9, 152.8, 150.3, 143.5, 141.0, 139.9, 139.3, 139.2, 128.9, 128.85, 128.82, 125.6, 125.56, 125.5, 125.4, 125.33, 125.3, 125.2, 124.4, 117.1, 105.6, 101.6, 92.0, 90.9, 32.9, 32.7, 23.2, 23.1, 14.3, 14.1, 7.6, 4.5. IR (KBr, cm^{-1}): 3118, 3078, 2956, 2931, 2874, 2198, 1975, 1698, 1603, 1465, 1446, 1271, 1238, 839. UV−vis (CH_2Cl_2, λ (ϵ)): 287 (87 000), 316 (43 000), 397 (35 000), 420 (40 000), 486 nm (9000 M^{-1} cm^{-1}). ES-MS (nature of the peak, relative intensity): *m/z* 1071.2 ([M − PF_6]$^+$, 100), 463.2 ([M − 2PF_6]$^{2+}$, 30). Anal. Calcd for $C_{52}H_{56}F_{12}N_6P_2RuSSi$: C, 51.35; H, 4.64; N, 6.91. Found: C, 51.07; H, 4.30; N, 6.64.

RuT_1. A solution of KF (12 mg, 0.19 mmol) in H_2O (3 mL) was added to a solution of **RuT_1(TES)** (50 mg, 0.04 mmol) in THF (5 mL) and EtOH (5 mL). The mixture was stirred for 5 h, and then the solvent was evaporated under vacuum. The residue was treated with a saturated solution of KPF_6 and extracted with dichloromethane. The organic extracts were washed with water and dried over absorbent cotton. The solvent was removed by rotary evaporation. The residue was purified by recrystallization in a mixture of dichloromethane and methanol to give 43 mg (94%) of **RuT_1** as an orange solid. ^{1}H NMR (400.1 MHz, $(CD_3)_2CO$): δ 8.85−8.81 (m, 6H), 8.27−8.18 (m, 8H), 8.08−8.03 (m, 4H), 7.64−7.57 (m, 4H), 7.26 (s, 1H), 4.13 (s, 1H), 2.64 (t, 2H, ^3J = 7.5 Hz), 2.55 (t, 2H, ^3J = 7.5 Hz), 1.64−1.25 (m, 8H), 0.92 (t, 3H, ^3J = 7.5 Hz), 0.88 (t, 3H, ^3J = 7.5 Hz). ^{13}C NMR (100.6 MHz, $(CD_3)_2CO$): δ 158.23, 158.19, 158.1, 158.0, 157.3, 156.1, 155.0, 153.6, 153.2, 153.1, 152.82, 152.80, 150.3, 143.5, 141.4, 140.0, 139.2, 128.8, 125.6, 125.5, 125.46, 125.4, 125.36, 125.34, 125.3, 125.2, 123.7, 117.1, 92.0, 90.8, 87.1, 79.1, 32.9, 32.7, 23.2, 23.1, 14.3, 14.1. IR (KBr, cm^{-1}): 3269, 3118, 3073, 2955, 2929, 2860, 2197, 2116, 1974, 1698, 1603, 1591, 1465, 1446, 1273, 1242, 840. UV−vis (CH_2Cl_2, λ (ϵ)): 270 (81 000), 395 (27 000), 420 (32 000), 483 nm (8000 M^{-1} cm^{-1}). ES-MS (nature of the peak, relative intensity): *m/z* 957.2 ([M − PF_6]$^+$, 50), 406.2 ([M − 2PF_6]$^{2+}$, 100). Anal. Calcd for $C_{46}H_{42}F_{12}N_6P_2RuS$: C, 50.14; H, 3.84; N, 7.62. Found: C, 49.82; H, 3.64; N, 7.36.

RuT_2. $[Ru(bpy)_2Cl_2]\cdot 2H_2O$ (34 mg, 0.07 mmol) was added to a mixture of 5,5′-bis[(3,4-dibutyl-5-iodothienyl)ethynyl]-2,2′-bipyridine (**T_2**, 50 mg, 0.06 mmol) in EtOH (10 mL). The stirred mixture was heated at 90 °C for 12 h and then the solvent was evaporated under vacuum. The residue was treated with a saturated solution of KPF_6 and extracted with dichloromethane. The organic extracts were washed with water and dried over absorbent cotton. The solvent was removed by rotary evaporation. The residue was purified by chromatography on alumina, eluting with dichloromethane−hexane (v/v 50/50) to dichloromethane−methyl alcohol (v/v *99.5*/0.5), to give 86 mg (94%) of **RuT_2** as an orange solid. ^{1}H NMR (400.1 MHz, $(CD_3)_2CO$): δ 8.85−8.81 (m, 6H), 8.28−8.21 (m, 8H), 8.08−8.06 (m, 4H), 7.64−7.59 (m, 4H), 2.70 (t, 4H, ^3J = 7.5 Hz), 2.57 (t, 4H, ^3J = 7.5 Hz), 1.52−1.26 (m, 16H), 0.95 (t, 6H, ^3J = 7.0 Hz), 0.89 (t, 6H, ^3J = 7.0 Hz). ^{13}C NMR (100.6 MHz, $(CD_3)_2CO$): δ 158.2, 158.1, 156.5, 153.7, 153.2, 152.8, 149.8, 147.7, 140.0, 139.2, 128.9, 125.49, 125.45, 125.4, 124.6, 122.6, 92.7, 90.7, 80.5, 33.2, 32.7, 23.3, 23.1, 14.3, 14.1. IR (KBr, cm^{-1}): 3120, 3083, 2955, 2930, 2860, 2197, 1698, 1596, 1465, 1427, 1374, 1274, 1242, 839. UV−vis (CH_2Cl_2, λ (ϵ)): 288 (86 000), 448 nm (70 000 M^{-1} cm^{-1}). ES-MS (nature of the peak, relative intensity): *m/z* 1403.2 ([M − PF_6]$^+$, 100), 629.2 ([M − 2PF_6]$^{2+}$, 25). Anal. Calcd for $C_{58}H_{58}F_{12}I_2N_6P_2RuS_2$: C, 45.00; H, 3.78; N, 5.43. Found: C, 44.62; H, 3.39; N, 5.04.

RuT_4. $Pd(PPh_3)_4$ (4.3 mg, 3.7 × 10^{-3} mmol) was added to an argon-degassed solution of **T_1** (31 mg, 0.08 mmol), **RuT_2** (48 mg, 0.03 mmol) in CH_3CN (8 mL), and *i*-Pr_2NH (8 mL). The solution was heated at 60 °C for 12 h, and then the solvent was evaporated

(15) (a) Walters, K. A.; Trouillet, L.; Guillerez, S.; Schanze, K. S. *Inorg. Chem.* **2000**, *39*, 5496. (b) Liu, S. X.; Schanze, K. S. *Chem. Commun.* **2004**, 1510. (c) Ley, K. D.; Li, Y.; Johnson, J. V.; Powell, D. H.; Schanze, K. S. *Chem. Commun.* **1999**, 1749. (d) Wang, Y.; Liu, S.; Pinto, M. R.; Dattelbaum, D. M.; Schoonover, J. R.; Schanze, K. S. *J. Phys. Chem. A* **2001**, *105*, 11118. (e) Simon, J. A.; Curry, S. L.; Schmehl, R. H.; Schatz, T. R.; Piotrowiak, P.; Jin, X.; Thummel, R. P. *J. Am. Chem. Soc.* **1997**, *119*, 11012. (f) Baba, A. I.; Shaw, J. R.; Simon, J. A.; Thummel, R. P.; Schmehl, R. H. *Coord. Chem. Rev.* **1998**, *171*, 43. (g) Shaw, J. R.; Schmehl, R. H. *J. Am. Chem. Soc.* **1991**, *113*, 389.

(16) Goeb, S.; De Nicola, A.; Ziessel, R. *J. Org. Chem.* **2005**, *70*, 6802.

under vacuum. The residue was treated with a saturated solution of KPF_6 and extracted with dichloromethane. The organic extracts were washed with water and dried over absorbent cotton. The solvent was removed by rotary evaporation. The residue was purified by chromatography on alumina, eluting with dichloromethane−hexane (v/v 50/50) to dichloromethane−hexane (v/v 80/20), to give 55 mg (84%) of **RuT$_4$** as an orange solid. ^{1}H NMR (400.1 MHz, $(CD_3)_2CO$): δ 8.86−8.80 (m, 10H), 8.53 (d, 2H, ^3J = 8.0 Hz), 8.51 (d, 2H, ^3J = 8.0 Hz), 8.30−8.23 (m, 8H), 8.10−8.01 (m, 8H), 7.66−7.62 (m, 4H), 7.17 (s, 2H), 2.85−2.80 (m, 8H), 2.71 (t, 4H, ^3J = 7.5 Hz), 2.62 (t, 4H, ^3J = 7.5 Hz), 1.70−1.33 (m, 32H), 1.02−0.91 (m, 24H). ^{13}C NMR (100.6 MHz, $(CD_3)_2$-CO): δ 158.3, 156.8, 155.8, 154.9, 154.0, 153.4, 153.0, 152.3, 152.2, 150.4, 149.1, 149.0, 143.5, 140.4, 140.1, 139.8, 139.5, 139.4, 129.08, 129.05, 125.7, 125.6, 124.9, 124.1, 122.0, 121.9, 121.62, 121.58, 120.8, 118.9, 118.6, 95.3, 92.7, 92.5, 91.1, 88.8, 87.0, 33.19, 33.16, 33.0, 23.44, 23.41, 23.32, 23.27, 14.4, 14.3, 14.23, 14.19. IR (KBr, cm^{-1}): 2954, 2928, 2859, 2194, 2194, 1591, 1464, 1446, 839. UV−vis (CH_2Cl_2, λ (ϵ)): 287 (98 000), 380 (109 000), 469 nm (95 000 M^{-1} cm^{-1}). ES-MS (nature of the peak, relative intensity): *m*/*z* 1943.5 ([M − PF_6]$^+$, 100), 899.3 ([M − 2PF_6]$^{2+}$, 20). Anal. Calcd for $C_{110}H_{108}F_{12}N_{10}P_2RuS_4$: C, 63.23; H, 5.21; N, 6.70. Found: C, 63.43; H, 5.43; N, 6.76.

Spectroscopic Studies. Spectrophotometric grade solvents were purchased from Aldrich Chemicals Co. and used as received. Absorption and emission spectra were recorded using a Hitachi U3300 spectrophotometer and a fully corrected Yvon-Jobin Fluorolog Tau-3 spectrofluorimeter, respectively. Low-temperature emission spectra were taken using an Oxford Instruments Optistat DN cryostat operated by an Oxford Instruments temperature controller. Temperature-dependent emission spectra were collected from 120 K to room temperature at intervals of 5 K. The system was allowed to equilibrate for 10 min between each reading. Luminescence quantum yields were measured in N_2-purged acetonitrile relative to ruthenium(II) tris(2,2′-bipyridine), as a reference system.[17] High-temperature studies were made with a Harrick Scientific demountable optical cell with a path length of 1 mm. The sample was dissolved in deoxygenated acetonitrile or dispersed in dried KBr and pressed into a transparent disk. Luminescence lifetimes were recorded after excitation with a 5 ns laser pulse delivered at 532 nm. Decay traces were averaged and analyzed by conventional statistical methods. Solutions used for emission spectral measurements were optically dilute (absorbance at excitation wavelength = 0.08) and were used in conjunction with nonemissive glass cutoff filters. Deconvolution of the reduced spectral profiles into Gaussian components was made with the commercially available software PEAKFIT.[18]

Flash photolysis studies were made with an Applied Photophysics Ltd LKS60 instrument. Excitation was made with 5 ns pulses at 532 nm delivered with a frequency-doubled Q-switched Nd:YAG laser, while detection was made at 90° using a pulsed high-intensity Xe arc lamp. The signal was detected with a fast-response PMT after passage through a high-radiance monochromator. Transient differential absorption spectra were recorded point-by-point with 5 individual records being averaged at each wavelength. Kinetic measurements were made after 50 individual records were averaged using global analysis methods. The sample was purged with N_2 before use, and the absorbance at the excitation wavelength was adjusted to be 0.20.

Electrochemical studies employed cyclic voltammetry with a conventional 3-electrode system using a BAS CV-50W voltammetric analyzer equipped with a Pt microdisk (2 mm^2) working electrode and a platinum wire counter electrode. Ferrocene was used as an internal standard and was calibrated against a saturated calomel reference electrode (SCE) separated from the electrolysis cell by a glass frit presoaked with electrolyte solution. The solutions contained the electrode-active substrate ($\sim 1 \times 10^{-3}$ M) in solvent previously deoxygenated with dried nitrogen and with tetra-*n*-butylammonium hexafluorophosphate (0.1 M) as supporting electrolyte. The quoted half-wave potentials were reproducible to within ±15 mV.

Molecular dynamics simulations (MDS) were performed with INSIGHT-II[19] running on a Silicon Graphics O2 workstation. Structures were drawn in the Builder module and partial charges were assigned using the ESFF force field.[20] Energy minimization was carried out with the Discover_3 module using the conjugate gradient method with a cutoff of 9.5 Å until the maximum derivative was less than 0.0005 kcal/Å. The energy-minimized geometries were used as the starting points for the MDS studies. Each MDS run consisted of an initial 10 ps of equilibration using the velocity-scaling method, followed by 100 ps of production dynamics. During the latter stage, the temperature averaged 300 K with a standard deviation of 4.8 K. Data points were sampled each 10 fs of simulation time.

Results and Discussion

Synthesis. Complexes **RuT$_1$(TES)** and **RuT$_2$** were prepared in excellent yields (>90%) by a classical protocol using the substituted 2,2′-bipyridine ligands **T$_1$(TES)** and **T$_2$** and with $Ru(bipy)_2Cl_2 \cdot 2H_2O$[21] acting as the metal precursor under polar conditions (Scheme 1). Deprotection of the TES group is straightforward in the presence of KF in protic conditions and afforded **RuT$_1$** in excellent yield. Synthesis of **RuT$_4$** required cross-coupling of the monoethynyl bipyridine ligand **T$_1$** with complex **RuT$_2$**, promoted by palladium(0) in the presence of acetonitrile because this solvent is needed to solubilize the starting material. Di-isopropylamine was used to neutralize the nascent HI acid. All complexes were purified by chromatography and recrystallized from appropriate solvents. Purity and structural assignments were addressed by NMR spectroscopy, mass spectrometry, and elemental analysis. Complexes have been purified according to the standard procedures used in this field including careful column chromatography and double recrystallization from suitable solvents. Three spectroscopic techniques are used to check the purity of each compound. Electrospray mass spectroscopy and proton and carbon NMR guaranties the absence of impurities. As a proof of purity, we have included the proton NMR of all three complexes as Figures 1 and 2. The proton traces are given below and unambiguously prove that the present complexes are pure enough to perform sophisticated optical spectroscopy. The slight imbalance between the found and calculated elemental analysis is probably caused by residual solvent; it does not mean that luminescent impurities are present.

It should be mentioned that other ruthenium(II) poly(pyridine) complexes bearing thiophene residues have been

(17) Crosby, G. A.; Demas, J. N. *J. Am. Chem. Soc.* **1971**, *93*, 2841.
(18) *PEAKFIT*, version 4.0; Jandel Scientific Corp.: Corte Madera, CA.
(19) *INSIGHT-II*; Accelrys Software Inc.: San Diego, CA.
(20) Shi, S.; Yan, L.; Yang, Y.; Fisher-Shaulsky, J.; Thacher, T. *J. Comput. Chem.* **2003**, *24*, 1059.
(21) Sullivan, B. P.; Salmon, D. J.; Meyer, T. J. *Inorg. Chem.* **1978**, *17*, 3334.

Scheme 1[a]

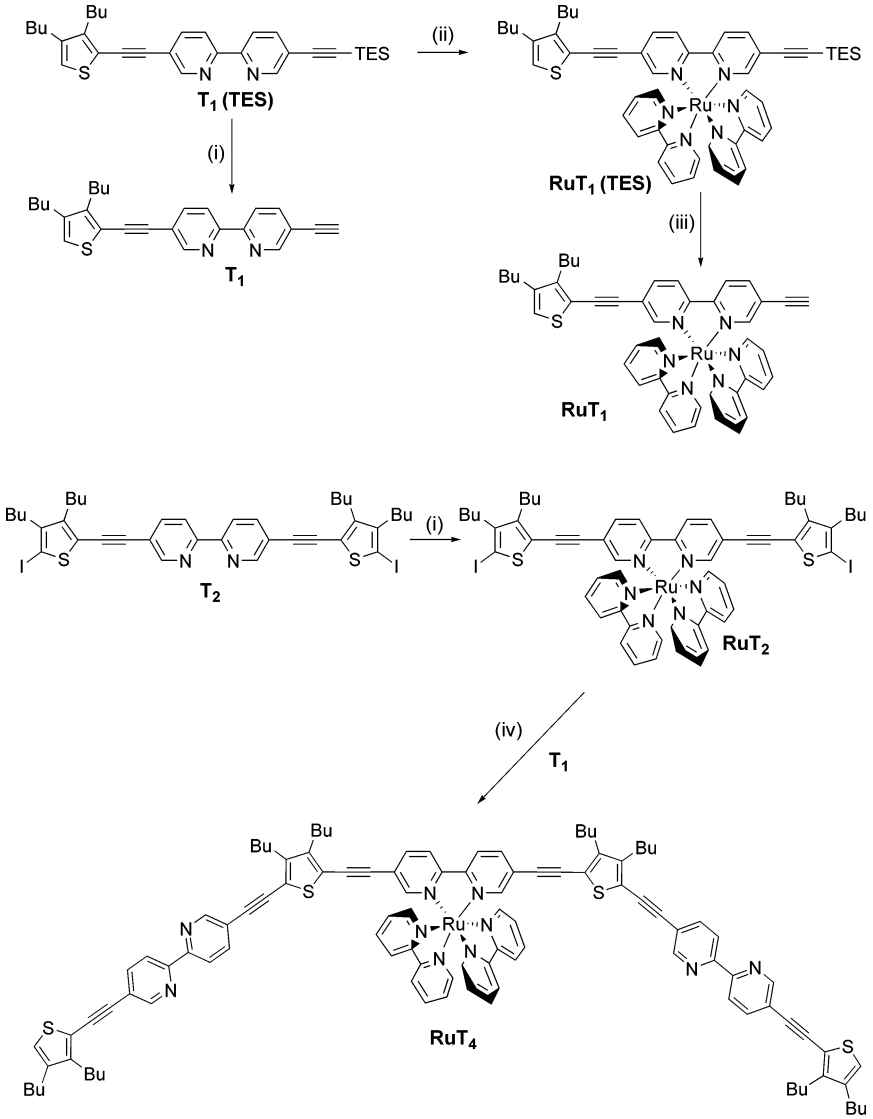

[a] Key: (i) KF, H_2O, THF, MeOH, 84%; (ii) $[Ru(bpy)_2Cl_2]\cdot 2H_2O$, EtOH, 90 °C, compound **RuT_1(TES)** 82%, compound **RuT_2** 94%; (iii) KF, H_2O, THF, EtOH, 94%; (iv) $Pd(PPh_3)_4$, CH_3CN, *i*-Pr_2NH, 60 °C, 84%. TES accounts for triethylsilylacetylene.

reported in the literature.[22] The present series of complexes is intended to provide a systematic extension of the π-conjugation length of the substituent attached to one of the 2,2′-bipyridine residues. The specific aim of the investigation is to establish if π,π^*-excited states localized on the substituted ligand make a significant contribution to the triplet manifold.[15] In particular, this requires a proper identification of the nature of the lowest-energy excited triplet state.

Electrochemistry. The electrochemical properties of the complexes were characterized by cyclic voltammetry in CH_3CN solution. Table 1 lists the half-wave potentials (relative to SCE, using ferrocene as internal reference) for the waves that were observed in the +1.6 to −2.1 V window. For each complex, a single, reversible anodic wave was observed around +1.36 V which is attributed to the Ru(II/III) couple.[23] Note that these half-wave potentials are 90 mV more anodic than that found for $[Ru(bpy)_3]^{2+}$, and this reflects the σ-withdrawing effect of the ethynylthiophene substituents.[24] The absence of a more pronounced effect is possibly counter balanced by the two dibutylthiophene donor groups. Interestingly, the second, irreversible anodic peak is likely caused

(22) (a) Harriman, A.; Mayeux, A.; De Nicola, A.; Ziessel, R. *Phys. Chem. Chem. Phys.* **2002**, *4*, 2229. (b) Encinas, S.; Flamigni, L.; Barigelletti, F.; Constable, E. C.; Housecroft, C. E.; Schofield, E. R.; Figgemeier, E.; Fenske, D.; Neuburger, M.; Vos, J. G.; Zehnder, M. *Chem.—Eur. J.* **2002**, *8*, 137. (c) Goeb, S.; De Nicola, A.; Ziessel, R.; Sabatini, C.; Barbieri, A.; Barigelletti, F. *Inorg. Chem.* **2006**, *45*, 1173. (d) Weldon, F.; Hammarstroem, L.; Mukhtar, E.; Hage, R.; Gunneweg, E.; Haasnoot, J. G.; Reedijk, J.; Browne, W. R.; Guckian, A. L.; Vos, J. G. *Inorg. Chem.* **2004**, *43*, 4471. (e) Suzuki, T.; Kuchiyama, T.; Kishi, S.; Kaizaki, S.; Takagi, H. D.; Kato, M. *Inorg. Chem.* **2003**, *42*, 785. (f) Barbieri, A.; Ventura, B.; Flamigni, L.; Barigelletti, F.; Fuhrmann, G.; Baeuerle, P.; Goeb, S.; Ziessel, R. *Inorg. Chem.* **2005**, *44*, 8033. (g) Henry, W.; Browne, W. R.; Ronayne, K. L.; O'Boyle, N. M.; Vos, J. G.; McGarvey, J. J. *J. Mol. Struct.* **2005**, *735*, 123. (h) Houarner, C.; Blart, E.; Buvat, P.; Odobel, F. *Photochem. Photobiol. Sci.* **2005**, *4*, 200. (i) Etienne, S.; Beley, M. *Inorg. Chem. Commun.* **2006**, *9*, 68.

(23) Grosshenny, V.; Harriman, A.; Romero, F. M.; Ziessel, R. *J. Phys. Chem.* **1996**, *100*, 17472.

(24) Liu, Y.; De Nicola, A.; Reiff, O.; Ziessel, R.; Schanze, K. S. *J. Phys. Chem. A* **2003**, *107*, 3476.

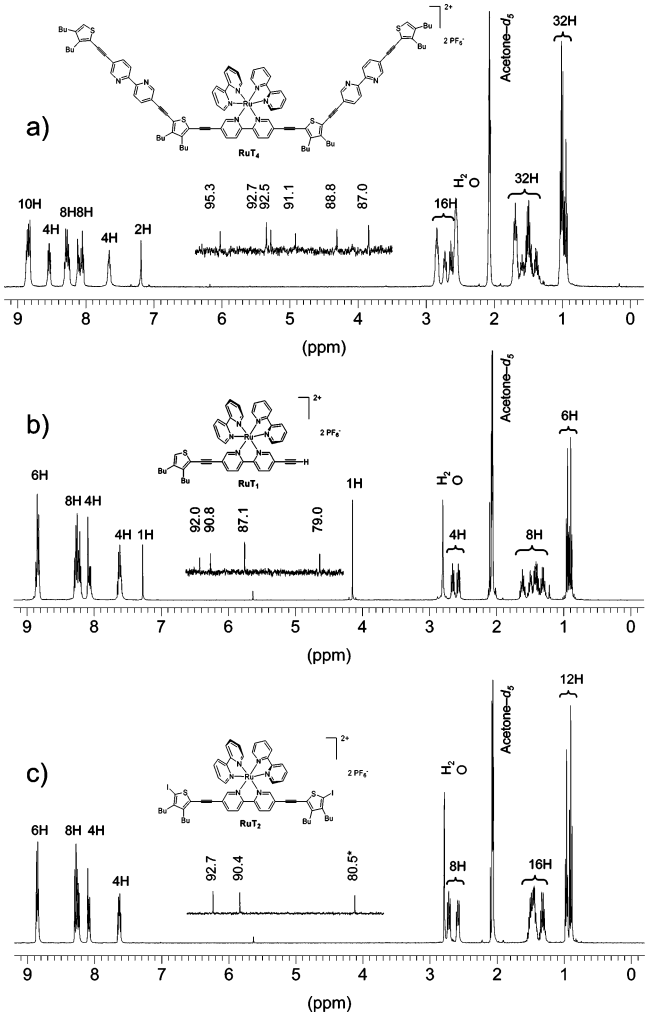

Figure 1. Proton NMR spectra recorded for the three complexes in dilute acetone-d_6 solution. The expanded ethynyl part of the carbon NMR spectra recorded for the three complexes in dilute acetone-d_6 solution is provided in the inset.

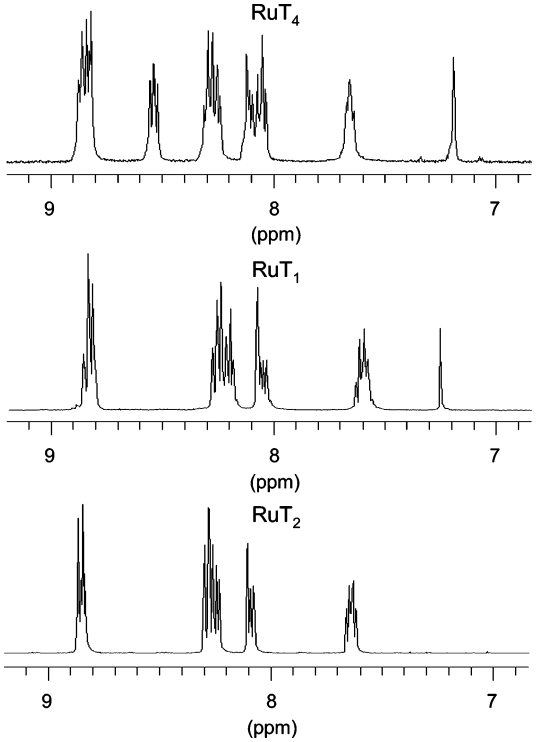

Figure 2. Expanded aromatic proton NMR spectra recorded for the three complexes in dilute acetone-d_6 solution.

Table 1. Electrochemical Properties of the Various Complexes in Solution[a]

	E°′ (ox, soln) V, ΔE_p (mV)[b]	E°′ (red, soln) V, ΔE_p (mV)[c]
RuT$_1$	1.35 (60), 1.67 (irrev), 1e	−1.01 (60), −1.50 (70), −1.72 (70)
RuT$_2$	1.36 (60), 1.66 (irrev)[d], 2e	−0.96 (70), −1.43 (70), −1.70 (irrev)[d]
RuT$_4$	1.36 (60), 1.64 (irrev)[d], 2e	−0.95 (60), −1.36 (70), −1.70 (irrev)[d]
$[Ru(bipy)_3]^{2+}$	1.27 (60)	−1.35 (60), −1.54 (70), −1.79 (70)

[a] Electrolyte was 0.1 M $TBAPF_6$/anhydrous CH_3CN, complex concentration 1−1.5 mM at room temperature. All potentials (±10 mV) are reported in V vs Pt^0 pseudoreference electrode and using Fc^+/Fc as internal reference (0.38 V, ΔEp = 70 mV). For irreversible processes (irrev), the anodic or cathodic peak potentials are given. [b] Metal-based oxidation. [c] Successive ligand-localized reductions; the first reduction occurs at the substituted bipy unit. [d] Overlap with a stripping peak.

by the oxidation of the peripheral dibutylthiophene unit.[25] We note that for **RuT$_2$** and **RuT$_4$** the height of the irreversible peak is twice that found for **RuT$_1$**, as might be expected on the basis of their relative chemical compositions.

Each complex exhibits at least three well-resolved waves in the cathodic branch of the voltammograms that can be attributed to successive reduction of the substituted and parent 2,2′-bipyridine ligands. In some cases, strong adsorption of the complex onto the electrode surface prevented accurate determination of the half-wave potential. The entries in Table 1 are organized according to the assignment as to which bipyridine ligand is reduced at the listed potential. For each of the complexes, the first reduction step is shifted to a more positive potential than that for $[Ru(bpy)_3]^{2+}$. This feature clearly indicates that the first reduction is localized on the ethynyl-substituted bipyridine ligand. In the case of **RuT$_1$**, the first reduction is facilitated by 340 mV compared to $[Ru(bpy)_3]^{2+}$ because of the presence of iodothiophene, whereas the substitution by an additional thiophene fragment, as in **RuT$_2$** and **RuT$_4$**, facilitates this reduction by a further 50 mV. An increase in the size of the substituted ligand, by the addition of two bipyridine/ethynylthiophen fragments in **RuT$_4$**, slighly perturbs the first reduction process. The additional parent bipyridine fragments in **RuT$_4$** are not resolved in the voltammograms because of overlap with adsorption/desorption peaks at very cathodic potentials.

Photophysical Studies. Absorption spectra recorded for the three complexes in acetonitrile solution are shown in Figure 3. In each case, the unsubstituted 2,2′-bipyridine ligands can be recognized by their characteristic absorption band centered at about 290 nm.[26] The substituted 2,2′-

(25) Barbieri, A.; Ventura, B.; Barigelletti, F.; De Nicola, A.; Quesada, M.; Ziessel, R. *Inorg. Chem.* **2004**, *43*, 7359.

(26) (a) De Armond, M. K.; Carlin, C. M. *Coord. Chem. Rev.* **1981**, *36*, 325. (b) Balzani, V.; Juris, A.; Venturi, M.; Campagna, S.; Serroni, S. *Chem. Rev.* **1996**, *96*, 759. (c) Juris, A.; Balzani, V.; Barigelletti, F.; Campagna, S.; Belser, P.; von Zelewsky, A. *Coord. Chem. Rev.* **1988**, *84*, 85.

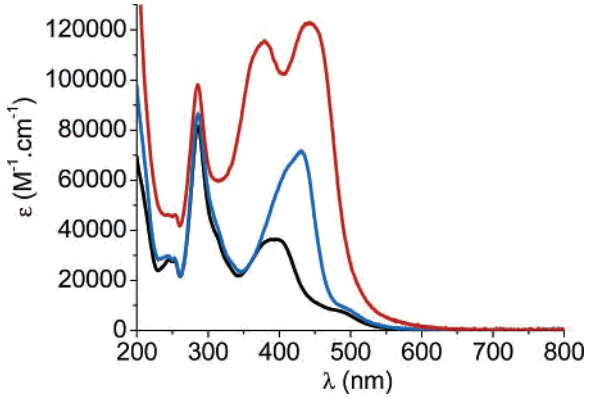

Figure 3. Absorption spectra recorded for the three complexes in dilute acetonitrile solution: **RuT$_1$** (black), **RuT$_2$** (blue), and **RuT$_4$** (red).

bipyridine ligand absorbs at longer wavelength and tends to dominate the spectrum, at least for the longer ligands. Thus, the π,π^*-transitions associated with the substituted ligand in **RuT$_1$** are seen in the region between 300 and 430 nm. These transitions are more intense for **RuT$_2$** and appear over the region from 340 to 460 nm. Since the only difference between these two complexes concerns the additional thiophene residue present in **RuT$_2$**, it follows that the terminal thiophene units form part of the conjugated pathway. For the extended system, **RuT$_4$**, these π,π^*-transitions are intensified further[27] and appear as two well-resolved bands centered at 380 and 460 nm. The expected metal-to-ligand charge-transfer (MLCT) transitions[26] involving the metal complex can be seen at 490 and 495 nm, respectively, for **RuT$_1$** and **RuT$_2$**. Relative to the parent complex, $[Ru(bipy)_3]^{2+}$ (bipy = 2,2′-bipyridine),[28] these MLCT bands are red shifted and somewhat intensified. The spin-allowed MLCT transition for **RuT$_4$** cannot be resolved from the more intense π,π^*-bands associated with the substituted bipy ligand. Such behavior is a common feature of metal poly(pyridine) complexes bearing fully conjugated ligands.[1,2] However, the corresponding spin-forbidden MLCT transitions can be seen in each complex as a weak tail stretching toward 600 nm. For the more extended system, **RuT$_4$**, this latter band reaches as far as 640 nm.

Each of the metal complexes was found to luminesce in deoxygenated acetonitrile at room temperature (Figure 4). The emission maximum (λ_{LUM}) was red shifted with respect to the parent complex and dependent on the nature of the attached thiophene unit (Table 2). Increasing the conjugation length leads to a progressive increase in λ_{LUM} under these conditions. The corrected excitation spectra were found to match nicely with the corresponding absorption spectra over the entire spectral range. Emission quantum yields (Φ_{LUM}) were calculated with respect to the parent complex and found to decrease with increasing conjugation length of the substituted bipy ligand (Table 2). Even so, the derived Φ_{LUM} values remain somewhat comparable to that of the parent complex. In all cases, the time-resolved luminescence decay profiles were found to correspond to a single-exponential

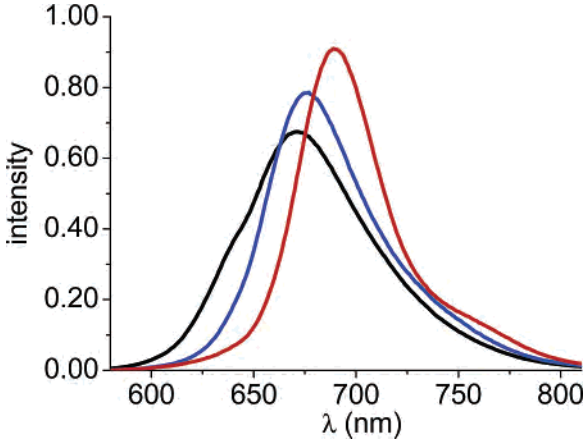

Figure 4. Luminescence spectra recorded for the three metal complexes in deoxygenated acetonitrile solution following excitation at 420 nm: **RuT$_1$** (black), **RuT$_2$** (blue), and **RuT$_4$** (red).

Table 2. Summary of the Photophysical Properties Measured for the Various Metal Complexes in Deoxygenated Acetonitrile Solution at Room Temperature

	λ_{LUM} (nm)	τ_{LUM} (ns)	Φ_{LUM}	k_{RAD} (s^{-1})	τ_T (ns)	k_{NR} (s^{-1})
$[Ru(bipy)_3]^{2+}$	627	970	0.062	6400	980	9.7×10^5
RuT$_1$	670	550	0.015	2730	550	18×10^5
RuT$_2$	677	770	0.011	1430	770	13×10^5
RuT$_4$	690	1400	0.0066	465	1450	7.1×10^5

process. The calculated emission lifetimes (τ_{LUM}) increase with increasing conjugation length; this is in direct contrast to the observed trend in quantum yields (Table 2). The measured lifetimes were independent of excitation and monitoring wavelength, insensitive to modest changes in concentration, and shortened upon the addition of molecular oxygen. The radiative rate constants (k_{RAD}) decrease sharply with increasing conjugation length. In part, this latter observation might be explained[29] in terms of fact that k_{RAD} should decrease with increasing λ_{LUM}, but the realization that τ_{LUM} shows the opposite trend suggests that the excited-state manifold might be complicated.

Laser flash photolysis studies were carried out in an effort to confirm the luminescence lifetimes. The metal complex in deoxygenated acetonitrile at room temperature was irradiated with a 5 ns laser pulse at 532 nm, and the resultant transient differential absorption spectrum recorded (Figure 5). In each case, the transient spectrum displays bleaching in the region where the substituted bipy ligand is known to absorb and absorption in the far-red region. The bleaching signal clearly corresponds to transient loss of the π,π^*-transition associated with the thiophene-based ligand. Both **RuT$_1$** and **RuT$_2$** exhibit sharp absorption bands around 470 and 510 nm, respectively, but **RuT$_4$** shows rather indistinct absorption stretching across the visible region and into the near-IR. These spectra differ markedly from that recorded for the parent complex[30] and known to be characteristic of the lowest-energy MLCT triplet state. However, it has been shown earlier[31] that the presence of an ethyne substitu-

(27) Pappenfus, T. M.; Mann, K. R. *Inorg. Chem.* **2001**, *40*, 6301.
(28) Nakamaru, K. *Bull. Chem. Soc. Jpn.* **1982**, *55*, 2697.
(29) Bixon, M.; Jortner, J.; Verhoeven, J. W. *J. Am. Chem. Soc.* **1994**, *116*, 7349.
(30) Carmichael, I.; Hug, G. L. *J. Phys. Chem. Ref. Data* **1986**, *15*, 1.

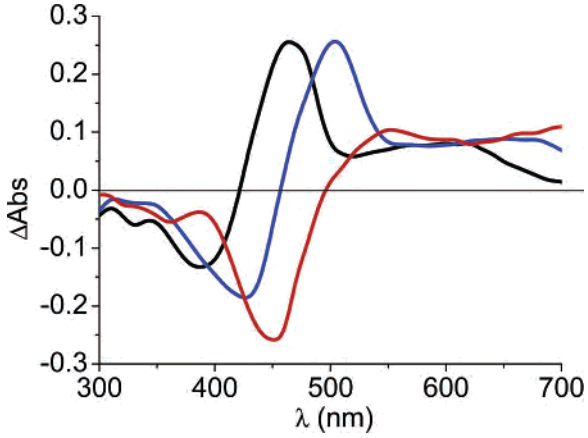

Figure 5. Transient differential absorption spectra recorded 270 ns after laser excitation ($\lambda = 532$ nm) of the metal complexes in deoxygenated acetonitrile solution: **RuT$_1$** (black), **RuT$_2$** (blue), and **RuT$_4$** (red).

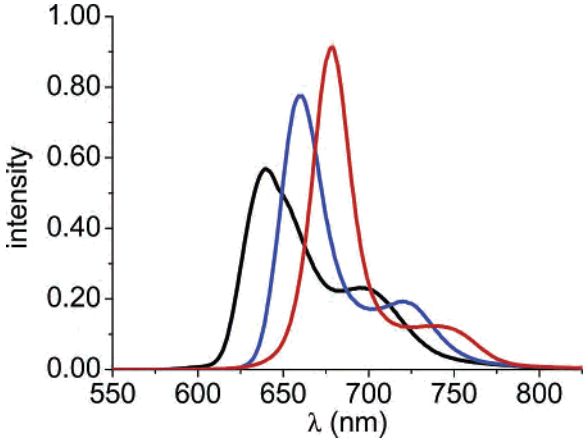

Figure 6. Luminescence spectra recorded for the three metal complexes in a deoxygenated butyronitrile glass at 77 K following excitation at 420 nm; **RuT$_1$** (black), **RuT$_2$** (blue), and **RuT$_4$** (red).

ent can have profound effects on the spectral properties of MLCT triplet states, and the differential spectra observed here should not be taken as being indicative of a π,π^*-triplet state localized on the substituted ligand.[32,33] The differences in the spectra are associated both with changes in the ground-state spectra and with variations in the properties of higher-lying triplet states, the latter being of particular importance for the longer analogue. Triplet lifetimes (τ_T) derived from the laser flash photolysis studies were in excellent agreement with those obtained from time-resolved emission spectroscopy (Table 2). In each case, the decay trace followed first-order kinetics and gave no hint of the presence of a second component. The addition of molecular oxygen increased the rate of decay.

Analysis of the Ambient-Temperature Emission Spectra. The luminescence spectra recorded for the thiophene-based metal complexes at ambient temperature are relatively broad and contain features clearly apparent on the high-energy side of the main transition; this is especially evident for **RuT$_1$**. Additional purification by TLC had no effect on the spectral profiles, but cooling of the mixture to 77 K in butyronitrile resulted in a marked sharpening of the spectrum (Figure 6). The features seen on the high-energy side disappear upon cooling. There was also a significant blue shift for each emission maximum; in a butyronitrile glass at 77 K, λ_{LUM} was found at 640, 660, and 680 nm, respectively, for **RuT$_1$**, **RuT$_2$**, and **RuT$_4$**. Such spectral shifts are well-known for metal complexes[34] and can be attributed to destabilization of the MLCT triplet state on moving from a polar solvent to a rigid glassy matrix.[35] This finding suggests that the observed emission arises from an MLCT triplet state. However, the higher-energy spectral features seen at ambient temperature require clarification.

The luminescence spectra recorded at room temperature were converted to wavenumber, reduced, and subjected to spectral deconvolution[6b] into the minimum number of Gaussian-shaped components. For both **RuT$_2$** and **RuT$_4$**, the entire spectral profile could be well reproduced as the sum of four Gaussian bands, with the three lower-energy bands sharing a common half width (Figure 7). The omission of any one band resulted in a very poor fit to the overall spectrum, while the addition of additional bands did not improve the quality of the fit by a noticeable amount, as determined from the residuals. The four Gaussian components can be considered to represent a vibrational progression of three bands, decreasing steadily in intensity, and a hot band situated at higher energy. The most intense band (E_{00}) corresponds to the 0,0 transition for the emission process, and the two lower-energy bands can be assigned, respectively, to a medium-frequency vibrational mode ($h\omega_M$) and a low-frequency vibrational mode ($h\omega_L$) coupled to nonradiative decay of the excited state. The higher-energy band assigned to hot emission lies some 850−900 cm^{-1} above the 0,0 transition (ΔE_H). The main parameters extracted from these spectral fits are collected in Table 3. The most noticeable feature of this analysis is that E_{00} moves toward lower energy with increasing conjugation length. The position of the hot emission band tracks this change in E_{00}.

The hot emission seen for **RuT$_1$** is more pronounced than for the other complexes, and in this case, the spectral profile cannot be properly described in terms of the four Gaussian components.[36] The best fit is obtained by adding an additional Gaussian component that appears to correspond to a vibrational band for the hot emission (Figure 8). In this analysis,

(31) Grosshenny, V.; Harriman, A.; Romero, F. M.; Ziessel, R. *J. Phys. Chem.* **1996**, *100*, 17472.
(32) (a) Benniston, A. C.; Grosshenny, V.; Harriman, A.; Ziessel, R. *Dalton Trans*. **2004**, 1227. (b) Benniston, A. C.; Harriman, A.; Romero, F. M.; Ziessel, R. *Dalton Trans*. **2004**, 1233.
(33) It should be recalled that the lowest-energy MLCT triplet state is formed by selective charge injection from the metal center to the substituted bipy ligand. This would have the effect of "bleaching" the π,π^*-transitions associated with the bipy ligand during the lifetime of the triplet state. The same effect would result if the triplet manifold involved the π,π^*-triplet state localized on the ligand. In both cases, the transient differential absorption spectra would be sensitive to the nature of the substituent.
(34) (a) Harrigan, R. W.; Hager, G. D.; Crosby, G. A. *Chem. Phys. Lett.* **1973**, *21*, 487.
(35) Worl, L. A.; Meyer, T. J. *Chem. Phys. Lett.* **1988**, *143*, 541.
(36) The spectrum could be fit to a total of four Gaussian bands, but the subsequent temperature-dependent analysis was inconsistent with a thermal equilibrium between two excited states. The addition of a vibronic component for the hot emission (of common half-width with the main hot band) provides a full description of the emission spectra at all temperatures and in both fluid and solid states.

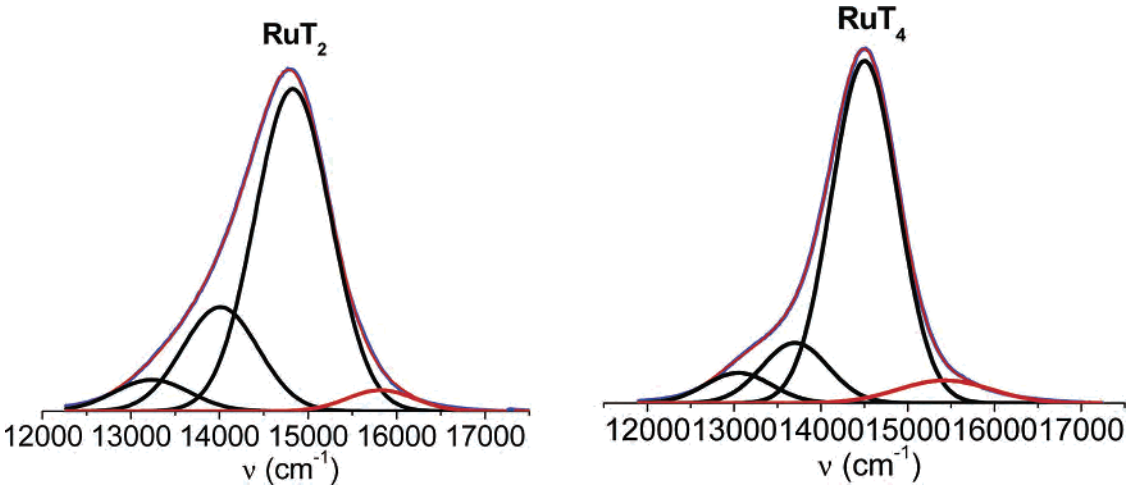

Figure 7. Deconvolution of the room-temperature emission spectra recorded for **RuT$_2$** (left-hand side) and **RuT$_4$** (right-hand side) at room temperature into the minimum number of Gaussian-shaped components. The normal vibrational progression is indicated in black, while the hot emission is represented in red. The fit to the entire spectrum is overlaid with the observed spectrum.

Table 3. Compilation of the Parameters Extracted from the Emission Spectral Curve-Fitting Routine Carried out for the Room-Temperature Spectra in Butyronitrile Solution and in a KBr Disk

parameters	medium	**RuT$_1$**	**RuT$_2$**	**RuT$_4$**
E_{00} (cm^{-1})	BuCN[a]	14 880	14 825	14 505
$h\omega_L$ (cm^{-1})	BuCN	820	815	800
$h\omega_M$ (cm^{-1})	BuCN	1655	1590	1455
ΔE_H (cm^{-1})	BuCN	780	1000	925
λ_T (cm^{-1})	BuCN	165	375	560
E_{00} (cm^{-1})	KBr[b]	15 040	14 830	14 245
$h\omega_L$ (cm^{-1})	KBr	800	760	785
$h\omega_M$ (cm^{-1})	KBr	1580	1490	1465
ΔE_H (cm^{-1})	KBr	660	1025	1040
λ_T (cm^{-1})	KBr	150	185	250

[a] Butyronitrile solution at 20 °C. [b] Transparent KBr disk at 20 °C.

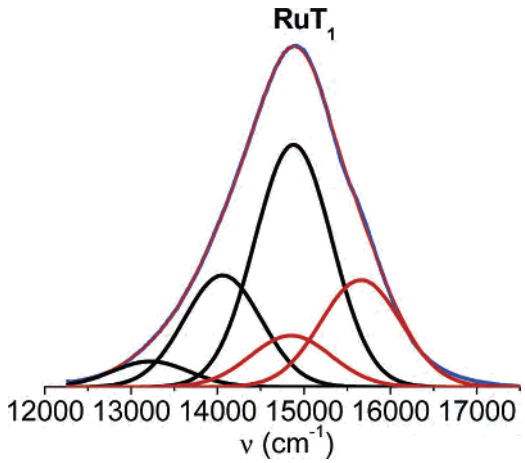

Figure 8. Deconvolution of the room-temperature emission spectra recorded for **RuT$_1$** at room temperature in butyronitrile solution into the minimum number of Gaussian-shaped components. The normal vibrational progression is indicated in black, while the hot emission is represented in red. The fit to the entire spectrum is overlaid with the observed spectrum.

the "normal" emission spectral profile follows the expected trend (Table 3), with E_{00} lying at slightly higher energy than that for **RuT$_2$** and with appropriate medium- and low-frequency modes coupled to nonradiative decay. The need to include an additional Gaussian suggests that the simpler fit found for **RuT$_2$** and **RuT$_4$** occurs because the hot emission is much less intense relative to the normal profile. The energy gap between the two Gaussian bands, these being of common half-width, used to describe the hot emission for **RuT$_1$** corresponds to a low-frequency vibrational mode of 810 cm^{-1}.

The same type of analysis was made for emission spectra collected for samples of the metal complexes dispersed in a transparent KBr disk (see Supporting Information). It was observed that the "normal" vibrational progression holds in the solid state, thereby eliminating the possibility that either the low- or medium-frequency vibrational modes arise from specific interactions with solvent molecules.[37] Hot emission is clearly apparent in the solid state, and as for fluid solution, this feature is significantly more pronounced for **RuT$_1$**. The derived parameters are collected in Table 3 and are closely comparable to those found by fitting the solution-phase spectra.

Temperature Effects on the Emission Spectra. The luminescence spectra were recorded in butyronitrile solution over the temperature range from 300 to 130 K: note that the solvent freezes at 162 K. In each case, there is a small increase in quantum yield with decreasing temperature, but even in the most extreme case, this represents no more than a 2-fold enhancement in the radiative probability. It is clear from these studies that the emitting species are not strongly coupled to a higher-energy state that promotes rapid decay to the ground state.[38] As the temperature decreases, there is a progressive loss of the hot emission and therefore a sharpening of the luminescence spectral profile. For each complex, there is an isoemissive point in fluid solution that confirms that the "normal" and "hot" emissions come from a thermally equilibrated mixture of triplet states.[39] This feature is lost as the solvent begins to freeze since the spectrum undergoes a slight blue shift, as noted earlier

(37) Caspar, J. V.; Meyer, T. J. *J. Am. Chem. Soc.* **1983**, *105*, 5583.
(38) (a) It is well established that an upper-lying metal-centered state makes a major contribution to deactivation of the MLCT triplet state for the corresponding terpyridine-based complexes (see ref 38b and c for leading references), but such effects are not important here. (b) Amini, A.; Harriman, A.; Mayeux, A. *Phys. Chem. Chem. Phys.* **2004**, *6*, 1157. (c) Benniston, A. C.; Chapman, G.; Harriman, A.; Mehrabi, M.; Sams, C. A. *Inorg. Chem.* **2004**, *43*, 4227.

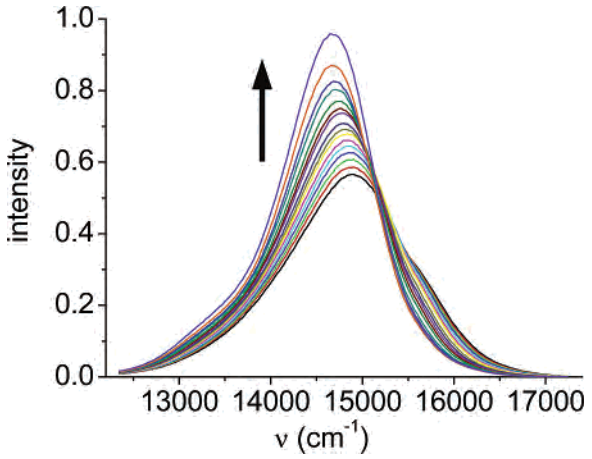

Figure 9. Effect of temperature on the luminescence spectral profile recorded for $\mathbf{RuT_1}$ in butyronitrile. Spectra were recorded from 290 to 140 K at intervals of 10 K. The arrow indicates the effect of decreasing temperature.

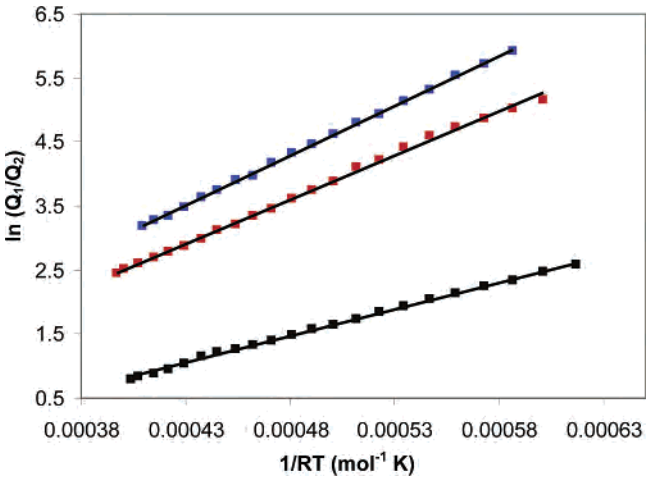

Figure 10. Boltzmann plots for the relative ratio of quantum yields for emission from the lower and upper states for $\mathbf{RuT_1}$ (black), $\mathbf{RuT_2}$ (blue), and $\mathbf{RuT_4}$ (red) in butyronitrile solution.

(Figure 6). The temperature effect is shown for $\mathbf{RuT_1}$ in Figure 9, and the corresponding spectral evolutions for $\mathbf{RuT_2}$ and $\mathbf{RuT_4}$ are given as part of the Supporting Information.

Equilibration between the two emitting species can be expressed in terms of a simple Boltzmann distribution law by considering the effect of temperature on the ratio of the quantum yields for normal (Q_1) and hot (Q_2) emission. The individual quantum yields were obtained by summation of the areas of the relevant Gaussian components before converting to relative values by normalization. It is seen that the ratio moves progressively in favor of the lower-energy species as the temperature decreases. The energy gap between the two emitting species was determined from the resultant linear Boltzmann plot (Figure 10) and was found to be in reasonable agreement with the spectroscopic energy gaps extracted from the emission spectral curve fitting routines (Table 4). Thus, the Boltzmann energy gaps (ΔE) were found to be 700, 1300, and 1150 cm^{-1} for $\mathbf{RuT_1}$, $\mathbf{RuT_2}$, and $\mathbf{RuT_4}$, respectively. Somewhat comparable ΔE values were obtained from the temperature dependence of the emission spectra recorded in a KBr disk (see Supporting Information), indicating that solvent plays no significant role in setting the differences in energy levels of these emitting states. At low temperature, only the lowest-energy triplet state emits.

The energy gaps (ΔE) derived from a Boltzmann-type analysis represent the difference in energy between the two emitting levels and are sensitive to the nature of the thiophene-based ligand. In making this analysis, we assumed that the energy gap is independent of temperature, but we have no obvious way to verify this proposition. Comparable ΔE values are obtained in solution and in a KBr disk, but they are considerably larger for $\mathbf{RuT_2}$ than for $\mathbf{RuT_1}$, although the difference in chemical composition is minor. There is an apparent discrepancy between these ΔE values and the corresponding energy gaps (ΔE_H) separating the E_{00} from the emission peak assigned to the hot band for both $\mathbf{RuT_2}$ and $\mathbf{RuT_4}$ (Table 4). A similar discrepancy is seen in the solid state. Furthermore, there is some suggestion that in solution ΔE_H is dependent on temperature (Table 4).

Table 4. Comparison of the Energy Gaps Determined from Boltzmann-Type Plots and by Emission Spectral Curve-Fitting Routines for the Various Metal Complexes

params	state	$\mathbf{RuT_1}$	$\mathbf{RuT_2}$	$\mathbf{RuT_4}$
ΔE (cm^{-1})	BuCN	700	1300	1150
ΔE_H (cm^{-1})	BuCN at 290 K	780	1000	925
ΔE_H (cm^{-1})	BuCN at 210 K	830	1100	970
ΔE (cm^{-1})	KBr	675	1200	1180
ΔE_H (cm^{-1})	KBr at 393 K	660	1000	1000
ΔE_H (cm^{-1})	KBr at 293 K	660	1025	1040

The Boltzmann-type energy gaps ΔE are calculated on the basis of the radiative rate constants for the emitting states being independent of temperature, which seems to be a reasonable assumption.[29] It is unlikely that the two states possess identical k_{RAD} values, and it should be noted that the individual quantum yields, Q_1 and Q_2, contain information about both the relative populations and k_{RAD} values for the two states. On the other hand, the ΔE_H values extracted from emission spectral curve-fitting routines refer specifically to the differences between the respective E_{00} values. The spectroscopic energy of an individual state is the sum of E_{00} and the reorganization energy that accompanies the deactivation process.[40] There is no obvious reason that the two emitting states should have identical reorganization energies, and therefore, the difference between ΔE and ΔE_H might reflect disparities in λ_T. Furthermore, the modest temperature dependence noted for ΔE_H in solution might also arise from modifications of λ_T.

Reorganization Energies. To shed more light on the nature of the emitting species, the emission spectra were used to calculate the size of the total reorganization energy (λ_T) accompanying deactivation of the excited state. The assump-

(39) The observation that the interconversion between the two emitting states is fully reversible is taken as strong evidence that the observed dual emission is not caused by the presence of an impurity. This conviction is strengthened by the realization that emission decay profiles were independent of monitoring wavelength across both bands. Excitation spectra recorded for the two bands were identical and fully consistent with the absorption spectrum. Subjecting the samples to repeated purification by TLC had no discernible effect on the spectral profiles or measured parameters.

(40) Marcus, R. A. *J. Phys. Chem.* **1990**, *94*, 4963.

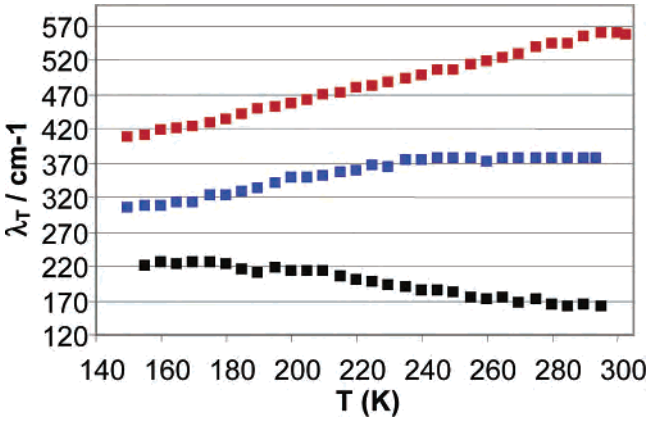

Figure 11. Effect of temperature on the reorganization energies derived for the complexes in butyronitrile solution by emission spectral curve fitting: **RuT$_1$** (black), **RuT$_2$** (blue), and **RuT$_4$** (red).

tion was made that the lowest-energy luminescent state possesses considerable charge-transfer character, this being validated by the spectral shifts upon freezing the solvent,[34,35] so that λ_T could be extracted from eq 1 after correcting the half-width ($\Delta\nu_{1/2}$) for any instrumental broadening. The derived values appropriate for room temperature are collected in Table 3 and are seen to increase with increasing conjugation length of the thiophene-based ligand. This latter effect is fully consistent with the substituted ligand facilitating electron delocalization at the triplet level.[41] Also in rough agreement with this possibility is the observation that λ_T increases with increasing temperature for both **RuT$_2$** and **RuT$_4$** (Figure 11). This temperature effect is reversed for **RuT$_1$**, where there is a slight decrease in λ_T with increasing temperature which cannot be easily explained. In a KBr disk, where internal motions are prohibited, λ_T is independent of temperature for all three complexes. We attribute the temperature dependence noted for the longer analogues to conformational motions that control the degree of π-electron delocalization throughout the extended ligands.[42]

$$\lambda_T = \frac{(\Delta\nu_{1/2})^2}{16\ln(2)\,k_B T} \qquad (1)$$

In principle, a similar treatment could be considered for the upper-lying triplet state, but this can be carried out only over a limited temperature range and is necessarily crude. Nonetheless, it is apparent that for all three complexes the reorganization energy for the upper-lying triplet state shows a more pronounced dependence on temperature than that of the lower-lying triplet. This behavior explains the observed effect of temperature on ΔE_H. For both **RuT$_2$** and **RuT$_4$**, λ_T for the upper-lying triplet is significantly larger than for the lower-lying triplet at any given temperature. This has the effect of bringing the actual triplet energy gaps ($\Delta E_T = \Delta E_H + \Delta\lambda_T$) much closer to the Boltzmann-type energy gaps, ΔE, for these two systems. The implication is that the upper-lying triplet state shows increased π-electron delocalization. For **RuT$_1$**, where dual emission is more prominent (Figure 8), the modest disparity between ΔE_H and ΔE cannot be explained solely in terms of changes in λ_T. A contributing factor in this system might be that the ratio of the individual quantum yields varies with temperature. Indeed, the results are easily explained in terms of a modest decrease in the Q_1/Q_2 ratio with decreasing temperature. This suggestion is not too unreasonable given that difference in λ_T values depends markedly on temperature.

Molecular Dynamics Simulations. Given the apparent importance of the reorganization energies in these complexes, a limited number of molecular dynamic simulations (MDS) were performed to gauge the extent of confomational motion available to the thiophene-based ligand in **RuT$_4$**. It was observed that there is essentially unrestricted rotation around the ethyne groups and that a statistical distribution of torsion angles abounds at each heterocycle. Furthermore, there was no obvious correlation between the total energy of the system and the average torsion angle at the heterocyclic residues, as might be expected if extended π-electron delocalization is important in the ground state. Within the many different families of conformations found for **RuT$_4$**, it was possible to identify two extreme structures as being relevant to the present discussion (see Supporting Information). These two geometries differ in terms of the extent of planarity between the bipy ligand and the appended thiophene residues. One conformation has these two units lying coplanar, presumably this structure being beneficial for extended electron delocalization, while the other family of structures has these two units lying orthogonal. The latter geometry will minimize electron delocalization and lead to a higher energy for the ligand-localized π,π^*-excited triplet state.[43]

Nature of the Emitting Species. Earlier work concerning binuclear ruthenium(II) bis(2,2′:6′,2″-terpyridine) complexes linked through a 2,5-diethynylated thiophene residue concluded that the lowest-energy, triplet-excited state was of MLCT parentage.[22a] The triplet energy was lowered with respect to the parent complex because of the electron-withdrawing effect of the ethyne group and because of electron delocalization at the triplet level. Comparable effects were reported for the corresponding binuclear complex with the terminals linked directly via a 2,5-thiophene residue.[22b] In contrast, the triplet manifold for a set of binuclear ruthenium(II) bis(2,2′:6′,2″-terpyridine) complexes bridged by oligomeric ($n = 1-5$) ethynylated thiophene residues was

(41) (a) Walters, K. A.; Premvardhan, L. L.; Liu, Y.; Peteanu, L. A.; Schanze, K. S. *Chem. Phys. Lett.* **2001**, *339*, 255. (b) Seneviratne, D. S.; Uddin, Md. J.; Swayambunathan, V.; Schlegel, H. B.; Endicott, J. F. *Inorg. Chem.* **2002**, *41*, 1502. (c) Browne, W. R.; Coates, C. G.; Brady, C.; Matousek, P.; Towrie, M.; Botchway, S. W.; Parker, A. W.; Vos, J. G.; McGarvey, J. J. *J. Am. Chem. Soc.* **2003**, *125*, 1706. (d) Damrauer, N. H.; McCusker, J. K. *J. Phys. Chem. A* **1999**, *103*, 8440. (e) Damrauer, N. H.; Boussie, T. R.; Devenney, M.; McCusker, J. K. *J. Am. Chem. Soc.* **1997**, *119*, 8253. (f) Turro, C.; Chung, Y. C.; Leventis, N.; Kuchenmeister, M. E.; Wagner, P. J.; Leroi, G. E. *Inorg. Chem.* **1996**, *35*, 5104.

(42) (a) Ruiz Delgado, M. C.; Casado, J.; Hernandez, V.; Lopez Navarrete, J. T.; Fuhrmann, G.; Bauerle, P. *J. Phys. Chem. B* **2004**, *108*, 3158. (b) Klokkenburg, M.; Lutz, M.; Spek, A. L.; van der Maas, J. H.; van Walree, C. A. *Chem.—Eur. J.* **2003**, *9*, 3544. (c) Viruela, P. M.; Viruela, R.; Ortí, E.; Casado, J.; Hernández, V.; López Navarrete, J. T. *J. Mol. Struct.* **2003**, *651*, 657. (d) Millefiori, S.; Alparone, A. *J. Chem. Soc., Faraday Trans.* **1998**, *94*, 25.

(43) (a) Rothe, C.; Brunner, K.; Bach, I.; Heun, S.; Monkman, A. P. *J. Chem. Phys.* **2005**, *122*, 084706. (b) Monkman, A. P.; Burrows, H. D. *Synth. Met.* **2004**, *141*, 81.

reported to comprise a mixture of MLCT and ligand-centered (LC) states.[25] These latter triplet states were described as π,π^*-states localized on the bridging ligand and their main effect was to promote nonradiative decay to the ground state. The conclusion derived from these particular studies is that the π,π^*-triplet is at lower energy than the MLCT triplet, at least for the more extended bridges. The same mixture of MLCT and π,π^*-triplet states was reported for binuclear ruthenium(II) tris(2,2′-bipyridine)-based complexes bridged by ethynylene-terminated oligothiophenes[22c] and for the corresponding system having a single thiophene residue in the bridge.[22g] Mixed-metal (M = Ru^{II}/Os^{II}) tris(1,10-phenanthroline)-based complexes lacking the connecting ethyne group were reported[14a] to display fast triplet energy transfer along the molecular axis. The first step in the transfer process was believed to involve injection of triplet energy into the thiophene-based bridge, which was situated at lower energy than the donor. Similar conclusions have been raised[8d] for certain heterodinuclear Ru^{II}/Ir^{I} complexes bridged by *para*-phenylene spacers, but here, the triplet energy of the donor is increased to a relatively high value. In the case of the corresponding Ru^{II}/Os^{II} binuclear complexes[44] it seems clear that the triplet localized on the bridge lies at higher energy than the donor triplet.

The photophysical properties of other ruthenium(II) poly(pyridine) complexes bearing conjugated substituents have been interpreted in terms of both MLCT and LC excited-triplet states. These LC states could be π,π^*-triplets localized on the conjugated organic backbone[15] or intramolecular charge-transfer states[2,15a] involving donor groups on the bridge and with the coordinated poly(pyridine) ligand acting as acceptor. For the thiophene-based complexes described herein, there is no evidence for the involvement of intramolecular charge-transfer states; note, the substituted ligand does not contain an appropriate electron donor.[45] The luminescence properties, and all the parameters derived from spectral curve fitting, are fully consistent with the lowest-energy excited-triplet state being of MLCT character. This is true in both fluid and solid states and at all temperatures studied. Furthermore, there is no indication for a low-energy π,π^*-triplet state that interacts with the MLCT triplet. Variations in the photophysical properties as the conjugation length increases can be explained by conventional treatments, without resorting to the involvement of additional triplet states.

Thus, for the lowest-energy triplet state, the effect of increased π-electron conjugation in the thiophene-based ligand is to decrease E_{00} and Φ_{LUM} while increasing both λ_T and τ_{LUM}. Charge injection at the triplet level occurs from the metal center to the substituted ligand. The more extended ligands show the greater propensity to delocalize the promoted electron, and this has a marked effect on the reorganization energy. This latter term is dominated by changes in nuclear coordinates, as shown by comparing solution and solid-state media. The trend in λ_T follows the order $\mathbf{RuT_1} < \mathbf{RuT_2} < \mathbf{RuT_4}$. The increased nuclear distortion also has the effect of decreasing E_{00} since the potential energy surfaces for ground and excited states will become more displaced as the degree of electron delocalization increases.[46] Additional consequences of the increased electron delocalization are a marked decrease in k_{RAD} and a decrease in the rate constant (k_{NR}) for the nonradiative decay of the excited triplet state. The effect on k_{RAD}, which has been noted before,[38c] can be traced to changes in the transition dipole moment.[29] However, the effect on k_{NR} is of a more subtle nature (Table 2).

The triplet energies of the thiophene-based compounds remain closely comparable to each other but considerably lower than that of the parent complex. The increased k_{NR} found for $\mathbf{RuT_1}$ relative to the parent (Table 2) is easily explained in terms of the energy-gap law[47] and by the need to include a low-frequency mode in deactivation of the former but not the latter.[6b,38b,38c] It is seen that k_{NR} decreases smoothly with increasing conjugation length (Table 2), and this is clearly related to the degree of π-electron delocalization at the triplet level.[46] Since E_T, $h\omega_M$, and $h\omega_L$ do not change significantly throughout the series, the electronic-vibronic coupling matrix element must decrease slightly with increasing conjugation length. Only a minor change is needed to account for the observed k_{NR} values.

There are a few other reports of dual emission from close-lying triplet-excited states for metal poly(pyridine) complexes, but these mostly refer to cases where the MLCT and π,π^*-triplet states lie at comparable energies.[48] The spectroscopic properties reported here for the two emitting species do not correspond to a mixture of MLCT and π,π^*-triplet states but appear to match the properties expected for MLCT triplet states. It is, in fact, well-known that many ruthenium(II) poly(pyridine) complexes possess a higher-lying MLCT triplet that can reside in thermal equilibrium with the lowest-energy MLCT triplet.[49] Furthermore, there are at least two cases of osmium(II) bis(2,2′:6′,2″-terpyridine) complexes[6b,50] that display dual emission from two MLCT triplets that differ

(44) (a) Barigelletti, F.; Flamigni, L.; Balzani, V.; Collin, J.-P.; Sauvage, J.-P.; Sour, A.; Constable, E. C.; Thompson, A. M. W. C. *J Chem. Soc., Chem. Commun*. **1993**, 942. (b) Barigelletti, F.; Flamigni, L.; Balzani, V.; Collin, J.-P.; Sauvage, J.-P.; Sour, A.; Constable, E. C.; Thompson, A. M. W. C. *J. Am. Chem. Soc*. **1994**, *116*, 7692.

(45) In contrast, intramolecular charge-transfer states are to be expected when the substituent is formed from an oligothiophene residue (see ref 27). The presence of ethyne groups and the restricted degree of oligomerization raises the energy of the charge-transfer state to above that of the MLCT triplet.

(46) (a) Strouse, G. F.; Schoonover, J. R.; Duesing, R.; Boyde, S.; Jones, W. E., Jr.; Meyer, T. J. *Inorg. Chem.* **1995**, *34*, 473. (b) Damrauer, N. H.; Weldon, B. T.; McCusker, J. K. *J. Phys. Chem. A* **1998**, *102*, 3382.

(47) Caspar, J. V.; Meyer, T. J. *J. Phys. Chem.* **1983**, *87*, 952.

(48) (a) Van Wallendael, S.; Rillema, D. P. *J. Chem. Soc., Chem. Commun*. **1990**, 1081. (b) Walters, K. A.; Ley, K. D.; Cavalaheiro, C. S. P.; Miller, S. E.; Gosztola, D.; Wasielewski, M. R.; Bussandri, A. P.; van Willigan, H.; Schanze, K. S. *J. Am. Chem. Soc*. **2001**, *123*, 8329. (c) Walters, K. A.; Ley, K. D.; Schanze, K. S. Dattelbaum, D. M.; Schoonover, J. R.; Meyer, T. J. *Chem. Commun*. **2001**, 1834. (d) Tyson, D. S,; Luman, C. R.; Zhou, X.; Castellano, F. N. *Inorg. Chem*. **2001**, *40*, 4063.

(49) (a) Allsop, S. R.; Cox, A.; Jenkins, S. H.; Kemp, T. J.; Tunstall, S. M. *Chem. Phys. Lett*. **1976**, *43*, 135. (b) Hartman, P.; Leiner, M. J. P.; Draxler, S.; Lippitsch, M. E. *Chem. Phys*. **1996**, *207*, 137. (c) Sykora, M.; Kincaid, J. R. *Inorg. Chem*. **1995**, *34*, 5852. (d) Harriman, A.; Mayeux, A.; Stroh, C.; Ziessel, R. *Dalton Trans*. **2005**, 2925.

(50) Lumpkin, R. S.; Kober, E. M.; Worl, L. A.; Murtaza, Z.; Meyer, T. J. *J. Phys. Chem*. **1990**, *94*, 239.

in terms of their spin−orbit coupling properties, with the higher-lying MLCT state retaining increased singlet character. The behavior reported here is entirely consistent with equilibration between two such MLCT triplets. Apart from their obvious difference in energy, these two MLCT states differ with respect to the extent of their interaction with the conjugated ligand. The experimental results are strongly indicative of the upper-lying state being more strongly coupled to the conjugated substituent.

The relative ordering of π,π^*- and MLCT-triplet states reported here for **RuT$_1$** and **RuT$_2$** agrees with that described earlier[24] for mononuclear Ru^{II} tris(2,2′-bipyridine) complexes bearing one or two ethynylatated thiophene residues. Indeed, the photophysical properties, with the exception of the noted dual emission, of these various mononuclear complexes are reasonably comparable, given the somewhat different experimental conditions. By all accounts,[51−61] however, we might expect that the π,π^*-triplet level for **RuT$_4$** should lie below the corresponding MLCT-triplet state, but this is not the case. The most likely reason for the π,π^*-triplet remaining at relatively high energy is that this state is highly localized over a small fragment of the ligand. Presumably, this situation arises because internal motions around the aryl units, most notably the vacant 2,2′-bipyridine groups, sever extended π-electron conjugation. In this respect, it is interesting to note that coordinating zinc(II) cations to the vacant 2,2′-bipyridine groups, thereby forcing the two pyridine rings into a coplanar arrangement, does not affect the emission spectral properties despite the obvious introduction of charge-transfer absorption bands in the near-UV region. It is not possible, on the basis of our experimental studies, to locate the energy of the π,π^*-triplet states in these complexes, but this is unlikely to be far removed from that of the MLCT triplet.

Acknowledgment. The Ministère de la Recherche et des Nouvelles Technologies is gratefully acknowledged for financial support of this work in the form of an Allocation de Recherche for S.G. We thank the EPSRC (EP/C007727/1), the CNRS, the University of Newcastle, and the Université Louis Pasteur for financial support of this work.

Supporting Information Available: Spectral overlays showing the effect of temperature on the emission profiles for **RuT$_2$** and **RuT$_4$** in butyronitrile and for all three complexes in KBr, deconvolution of the emission spectra recorded in KBr into Gaussian-shaped components, Boltzmann-type plots for KBr, and extreme conformations obtained from the MDS studies. This material is available free of charge via the Internet at http://pubs.acs.org.

IC060921W

(51) (a) Köhler, A.; Wilson, J. S.; Friend, R. H.; Al-Suti, M. K.; Khan, M. S.; Gerhard, A.; Bässler, H. *J. Chem. Phys.* **2002**, *116*, 9457. (b) Blatchford, J. W.; Gustafson, T. L.; Epstein, A. J. *J. Chem. Phys.* **1996**, *105*, 9214.
(52) Beljonne, D.; Wittmann, H. F.; Köhler, A.; Graham, S.; Younus, M.; Lewis, J.; Raithby, P. R.; Khan, M. S.; Friend, R. H.; Brédas, J. L. *J. Chem. Phys.* **1996**, *105*, 3868.
(53) Hertel, D.; Setayesh, S.; Nothofer, H.-G.; Scherf, U.; Müllen, K.; Bässler, H. *Adv. Mater.* **2001**, *13*, 65.
(54) Walters, K. A.; Ley, K. D.; Schanze, K. S. *Chem. Commun.* **1998**, 1115.
(55) Beljonne, D.; Shuai, Z.; Pourtois, G.; Brédas, J. L. *J. Phys. Chem. A* **2001**, *105*, 3899.
(56) Scaiano, J. C.; Redmond, R. W.; Mehta, B.; Arnason, J. T. *Photochem. Photobiol.* **1990**, *52*, 655.
(57) (a) Janssen, R. A. J.; Moses, D.; Sariciftci, N. S. *J. Chem. Phys.* **1994**, *101*, 9519. (b) Janssen, R. A. J.; Smilowitz, L.; Sariciftci, N. S.; Moses, D. *J. Chem. Phys.* **1994**, *101*, 1787.
(58) Zeng, Y.; Biczok, L.; Linschitz, H. *J. Phys. Chem.* **1992**, *96*, 5237.
(59) Xu, B.; Holdcroft, S. *J. Am. Chem. Soc.* **1993**, *115*, 8447.
(60) Beljonne, D.; Cornil, J.; Friend, R. H.; Janssen, R. A. J.; Brédas, J. L. *J. Am. Chem. Soc.* **1996**, *118*, 6453.
(61) (a) Swanson, L. S.; Shinar, J.; Yoshino, K. *Phys. Rev. Lett.* **1990**, *65*, 1140. (b) Bennati, M.; Grupp, A.; Bäuerle, P.; Mehring, M. *Mol. Cryst. Liq. Cryst.* **1994**, *256*, 751.